European Journal of Pharmaceutics and Biopharmaceutics 83 (2013) 16–24

Contents lists available at SciVerse ScienceDirect

European Journal of Pharmaceutics and Biopharmaceutics

journal homepage: www.elsevier.com/locate/ejpb

Research paper

Liquid crystalline phase nanodispersions enable skin delivery of siRNA

Fabiana Testa Moura de Carvalho Vicentini [a], Lívia Vieira Depieri [a], Ana Cristina Morseli Polizello [a], José Orestes Del Ciampo [a], Augusto César Cropanese Spadaro [a], Márcia C.A. Fantini [b], Maria Vitória Lopes Badra Bentley [a,*]

[a] Faculdade de Ciências Farmacêuticas de Ribeirão Preto, Universidade de São Paulo, Ribeirão Preto, SP, Brazil
[b] Instituto de Física, Universidade de São Paulo, Brazil

ARTICLE INFO

Article history:
Received 27 December 2011
Accepted in revised form 22 August 2012
Available online 23 September 2012

Keywords:
Nanodispersions
Liquid crystalline phase
Small interfering RNA
Topical delivery
Skin penetration

ABSTRACT

The ability of small interfering RNAs (siRNAs) to potently but reversibly silence genes *in vivo* has made them particularly well suited as a new class of drugs that interfere with disease-causing or disease-promoting genes. However, the largest remaining hurdle for the widespread use of this technology in skin is the lack of an effective delivery system. The aim of the present study was to evaluate nanodispersed systems in liquid crystalline phases that deliver siRNA into the skin. The proposed systems present important properties for the delivery of macromolecules in a biological medium, as they are formed by substances that have absorption-enhancing and fusogenic effects; additionally, they facilitate entrapment by cellular membranes due to their nano-scale structure. The cationic polymer polyethylenimine (PEI) or the cationic lipid oleylamine (OAM) were added to monoolein (MO)-based systems in different concentrations, and after dispersion in aqueous medium, liquid crystalline phase nanodispersions were obtained and characterized by their physicochemical properties. Then, *in vitro* penetration studies using diffusion cell and pig ear skin were carried out to evaluate the effect of the nanodispersions on the skin penetration of siRNA; based on these results, the nanodispersions containing MO/OA/PEI/aqueous phase (8:2:5:85, w/w/w/w) and MO/OA/OAM/aqueous phase (8:2:2:88, w/w/w/w) were selected. These systems were investigated *in vivo* for skin penetration, skin irritation, and the ability to knockdown glyceraldehyde 3-phosphate dehydrogenase (GAPDH) protein levels in animal models. The results showed that the studied nanodispersions may represent a promising new non-viral vehicle and can be considered highly advantageous in the treatment of skin disorders; they were effective in optimizing the skin penetration of siRNA and reducing the levels of the model protein GAPDH without causing skin irritation.

1. Introduction

RNA interference (RNAi) is an evolutionarily conserved process by which double-stranded small interfering RNAs (siRNAs) induce sequence-specific, post-transcriptional gene silencing. Unlike other mRNA targeting strategies, RNAi takes advantage of the physiological gene silencing machinery [1]. The discovery of RNAi and the observation that siRNAs largely evade the immune response have opened up new therapeutic opportunities. The ability of siRNAs to potently but reversibly silence genes *in vivo* has made them particularly well suited as a new class of drugs that interfere with disease-causing or disease-promoting genes. Clinical trials of siRNAs targeting the liver, kidney, lung, eye and skin are currently underway [2,3].

The skin is a uniquely attractive tissue for the investigation of RNAi therapeutic approaches due to its accessibility and the fact that there are a large number of diseases amenable to cutaneous gene mediation [4]. Several *in vitro* and *in vivo* studies have used the skin as a siRNA delivery route for the treatment of melanoma [5], rheumatoid arthritis [4], wounds [6], allergic skin diseases (such as contact hypersensitivity and atopic dermatitis [7]), and dominant genetic skin conditions, including pachyonychia congenita [8], alopecia areata [9] and psoriasis [10]. Therefore, topical delivery of siRNA can strategically modulate local gene expression in a variety of cutaneous disorders while avoiding systemic side effects [6]. Nevertheless, normal skin (especially the stratum corneum) represents a considerable barrier to topical nucleic acid delivery, and this obstacle poses a particular challenge for the delivery of siRNA because cellular- and tissue-level transport barriers must be overcome [11,12]. The clinical use of RNAi has been severely hampered by the lack of delivery systems for these molecules to target cell populations *in vivo* due to their instability, inefficient cell entry, and poor pharmacokinetic profile [13]. Thus,

* Corresponding author. Faculdade de Ciências Farmacêuticas de Ribeirão Preto, Universidade de São Paulo, Av. do Café, s/n, 14040-903 Ribeirão Preto, SP, Brazil. Tel./fax: +55 16 36024301.
E-mail address: vbentley@usp.br (M. Vitória Lopes Badra Bentley).

0939-6411/$ - see front matter © 2012 Elsevier B.V. All rights reserved.
http://dx.doi.org/10.1016/j.ejpb.2012.08.011

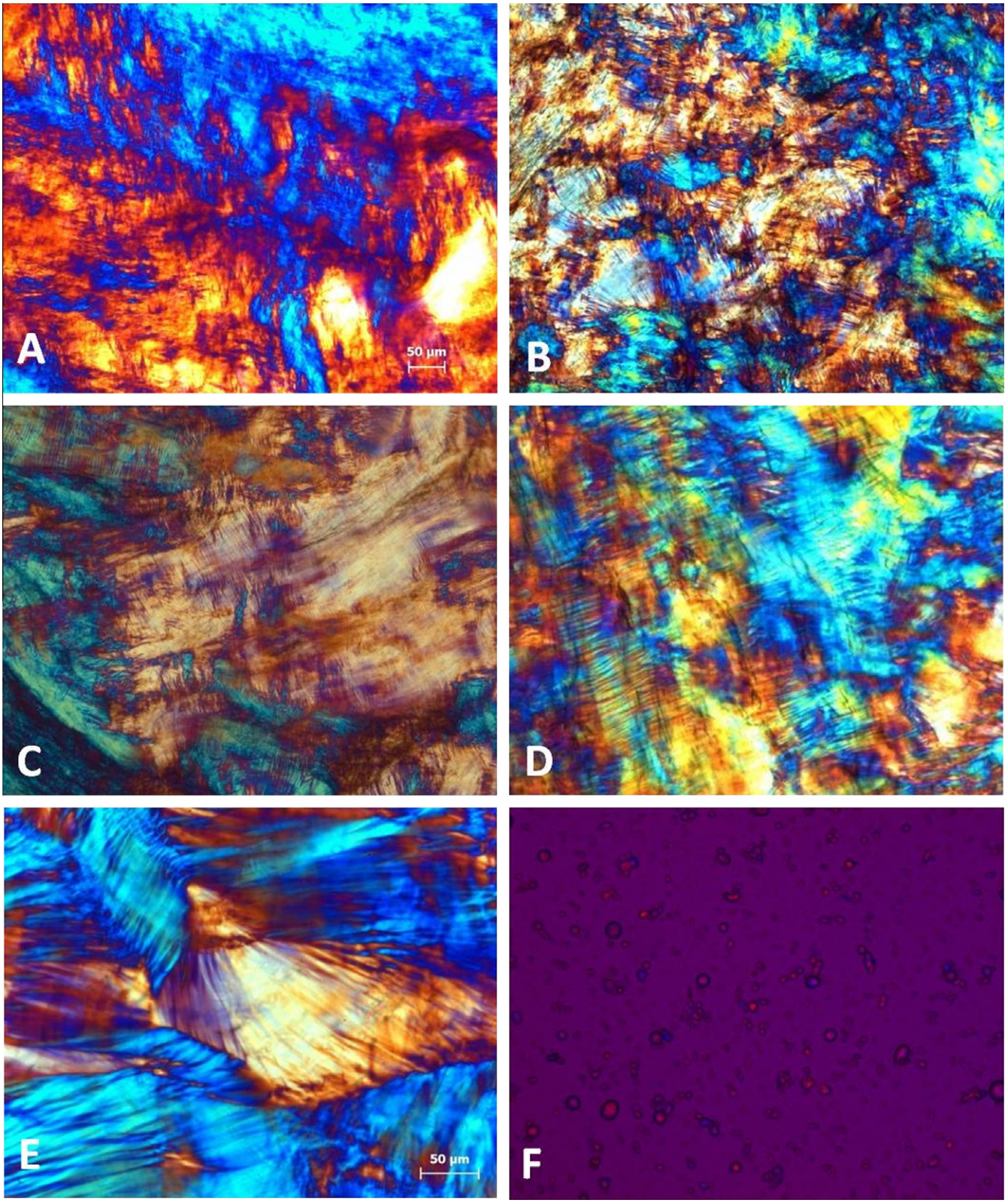

Fig. 1. Photomicrographs using polarized light microscopy. Hexagonal phase gel composed of (A) MO/PEI/aqueous phase (7:3:90, w/w/w), (B) MO/OAM/aqueous phase (9.5:0.5:90, w/w/w), (**C**) MO/OA/PEI/aqueous phase (8:2:2:88, w/w/w/w), and (D and E) MO/OA/OAM/aqueous phase (8:2:2:88, w/w/w/w). (F) Nanodispersion obtained after sonication (composed of MO/PEI/aqueous phase at 7:3:90, w/w/w). For panels A–D, a 20X objective was used, and for panels E and F, a 32X objective was uses. (For interpretation of the references to color in this figure legend, the reader is referred to the web version of this article.)

carrier systems are required to overcome these barriers, and delivery is a key determinant as to whether RNAi-based therapeutics will have clinical relevance [14,15].

In general, the ideal material for topical delivery of siRNA should be able to (i) bind and condense siRNA, (ii) overcome the barrier function of the stratum corneum [16], (iii) provide protection

Table 1
SAXS data for MO or MO/OA-based nanodispersions incorporated with different concentrations of PEI or OAM and with 2.5 μM siRNA.

Sample	q (nm^{-1})	d (nm)	Ratio	Mean lattice parameter (nm)	Structure
MO/PEI/Aqueous phase (9.6:0.4:90, w/w/w)	0.78	8.06	1:1		Cubic D
	1.03	6.10	1:1	a_H = 7.04 ± 0.01	Hexagonal
	1.10	5.71	$1:\sqrt{2}$	a_C = 8.10 ± 0.07	Cubic D
	1.33	4.72	$1:\sqrt{3}$		Cubic D
MO/PEI/Aqueous phase + siRNA (9.6:0.4:90, w/w/w)	0.78	8.06	1:1		Cubic D
	1.01	6.22	1:1	a_H = 7.18 ± 0.04	Hexagonal
	1.09	5.76	$1:\sqrt{2}$	a_C = 8.11 ± 0.04	Cubic D
	1.34	4.69	$1:\sqrt{3}$		Cubic D
MO/OAM/ Aqueous phase (9.6:0.4:90, w/w/w)	1.21	5.19	1:1		Hexagonal
	2.11	2.98	$1:\sqrt{3}$	a_H = 5.97 ± 0.01	Hexagonal
	2.43	2.59	$1:\sqrt{4}$		Hexagonal
MO/OAM/Aqueous phase + siRNA (9.6:0.4:90, w/w/w)	1.22	5.15	1:1		Hexagonal
	2.12	2.96	$1:\sqrt{3}$	a_H = 5.92 ± 0.03	Hexagonal
	2.46	2.55	$1:\sqrt{4}$		Hexagonal
MO/OA/PEI/ aqueous phase (8:2:1:89, w/w/w/w)	1.31	4.80	1:1	a_H = 5.57 ± 0.03	Hexagonal
	2.60	2.42	$1:\sqrt{4}$		Hexagonal
MO/OA/PEI/Aqueous phase + siRNA (8:2:1:89, w/w/w/w)	1.32	4.76	1:1	a_H = 5.50 ± 0.02	Hexagonal
MO/OA/OAM/Aqueous phase (8:2:2.5:87.5, w/w/w/w)	1.35	4.65	1:1		Hexagonal
	2.35	2.67	$1:\sqrt{3}$	a_H = 5.36 ± 0.02	Hexagonal
	2.70	2.33	$1:\sqrt{4}$		Hexagonal
MO/OA/OAM/Aqueous phase + siRNA (8:2:2.5:87.5, w/w/w/w)	1.37	4.59	1:1		Hexagonal
	2.36	2.66	$1:\sqrt{3}$	a_H = 5.31 ± 0.01	Hexagonal
	2.73	2.30	$1:\sqrt{4}$		Hexagonal

a_H: Mean lattice parameter of the hexagonal structure.
a_C: Mean lattice parameter of the cubic structure.
Cubic: D (Pn3m and Pm3n).
The results are represented as means ± mean standard error.

against degradation, (iv) direct siRNA to target cells, (v) facilitate its intracellular uptake, (vi) escape from endosome trafficking to the lysosome to reach the cell cytoplasm and avoid metabolism, and (vii) promote efficient gene silencing [17,18].

Carriers for siRNA delivery usually consist of cationic polymers, peptides, or lipids that form complexes with the nucleic acid, protecting it from nuclease attack and facilitating cell uptake through electrostatic interactions with negatively charged phospholipid bilayers or through specific targeting moieties [19].

Additionally, lyotropic liquid crystals, which can provide enhanced drug solubility, relative drug protection, and controlled release of drugs while avoiding substantial side effects, seem to be promising candidates as an alternative delivery means for various pharmaceuticals [20]. Liquid crystalline phases of monoolein were explored by Lopes et al. [21] to improve the skin penetration of a model peptide (cyclosporin A). The results, which demonstrated that the developed system increased the skin penetration of cyclosporin A both *in vitro* and *in vivo* without causing skin irritation, suggested the potential applicability of liquid crystalline nanodispersions as a safe and promising strategy for the topical delivery of several other macromolecules of dermatological interest [21].

Therefore, considering that the largest remaining hurdle for widespread use of siRNA technology in skin is the lack of an effective delivery system due to the low absorption of this hydrophilic macromolecule across the skin, and in view of the potentiality of liquid crystalline nanodispersions as topical carriers of macromolecules, the present study aimed to evaluate nanodispersions of liquid crystalline phases as non-viral vehicles to improve skin siRNA delivery.

To this end, the cationic polymer polyethylenimine (PEI), which is commonly used in gene delivery applications, or the cationic lipid oleylamine (OAM) were added to monoolein (MO)-based liquid crystalline nanodispersions. Then, the selected formulations were evaluated *in vivo* for the parameters of skin penetration, skin irritation, and ability to knockdown glyceraldehyde 3-phosphate dehydrogenase (GAPDH) protein levels in animal models, and their efficacies as siRNA delivery systems were compared.

2. Materials and methods

2.1. Materials

Monoolein (Myverol 18–99) was supplied by Quest (Norwich, NY, USA); branched PEI (25 kDa), oleic acid (OA), and OAM were obtained from Sigma (St. Louis, MO, USA); poloxamer 407 (Pluronic F127®) was obtained from BASF (Florham Park, NJ, USA); the GAPDH antibody was purchased from Santa Cruz Biotechnology (Santa Cruz, CA, USA); and the siRNAs used were scrambled siRNA (*Silencer* Negative Control #1 siRNA-Catalogue #AM4635) and fluorescently labeled siRNA targeting GAPDH (*Silencer* 6-carboxyfluorescein (FAM) GAPDH siRNA-Catalogue #AM4650), both purchased from Ambion (Austin, TX, USA). Fluorescently labeled siRNA (GAPDH siRNA-FAM) is commonly utilized for the easy monitoring of siRNA uptake by fluorescence microscopy along with siRNA-induced knockdown.

2.2. Preparation of test nanodispersions

Systems containing MO or MO/OA in the oil phase and 0.1 M Tris–HCl, pH 6.5, containing 1.5% (w/w) of poloxamer 407 in the aqueous phase were incorporated with different percentages (0.25–5%, w/w) of the cationic polymer PEI or the cationic lipid OAM. For this preparation, MO was melted (42 °C), and OA, PEI, or OAM were added with stirring. Immediately thereafter, the aqueous phase was added, and the resulting formulation was allowed to equilibrate at room temperature for 24 h. To obtain the dispersions, the gel with excess water was vortexed and sonicated (22.5 kHz) in an ice-bath for 2 min. Then, the siRNA was incorporated into the dispersions to a final concentration of 2.5 μM and left for 30 min at room temperature.

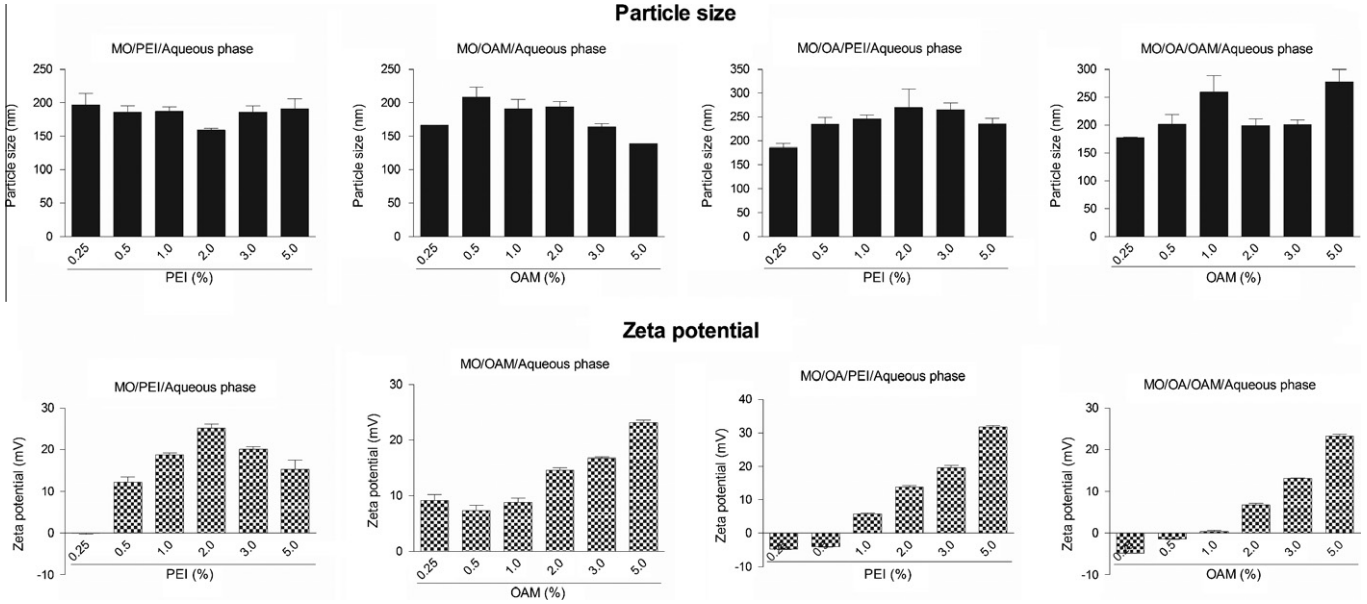

Fig. 2. Particle size (nm) and zeta potential of MO or MO/OA-based nanodispersions incorporated with different concentrations of PEI or OAM (0.25–5%) and with siRNA at 2.5 μM. The results are represented by means ± SEM (n = 3).

Table 2
Physicochemical properties of the selected nanodispersions incorporated with 10 μM siRNA[a].

Formulation	Diameter (nm)	Polydispersity	Zeta potential (mV)
MO/PEI/Aqueous phase (8:2:90, w/w/w)	159 ± 4	0.24 ± 0.03	25.1 ± 1.8
MO/OAM/Aqueous phase (9.75:0.25:90, w/w/w)	166.3 ± 0.9	0.23 ± 0.02	9.2 ± 1.8
MO/OA/PEI/Aqueous phase (8:2:5:85, w/w/w/w)	236 ± 17	0.38 ± 0.02	31.80 ± 0.60
MO/OA/OAM/Aqueous phase (8:2:2:88, w/w/w/w)	199 ± 17	0.26 ± 0.08	6.69 ± 0.60

[a] The data were compiled from three experiments ± mean standard error.

2.3. Characterization of test nanodispersions

2.3.1. Polarized light microscopy

The developed systems were characterized under a polarized light microscope (Axioplan 2 Image Pol microscope, Carl Zeiss, Oberkochen, Germany) before and after the sonication process used to disperse the bulk gel.

2.3.2. Small Angle X-ray Scattering (SAXS)

The liquid crystalline structure of the dispersed particles was analyzed by SAXS measurements performed at the Crystallography Laboratory of the Physics Institute-USP using Nanostar equipment (Bruker). The dispersions were placed in cylindrical glass capillaries with an internal diameter of 1.5 mm. The scattering curve of a single capillary was used as blank/parasite scattering, which was removed from the sample intensities after transmission correction. The X-ray tube was operated at 40 kV and 30 mA, generating Cu Kα radiation, $\lambda = 0.1540$ nm, monochromatized by Göbel mirrors. A point focus beam at the sample holder, approximately 1 mm diameter, was produced by the X-ray optics. The acquisition time of each scattering curve was 3 h, and a two-dimensional filament detector was utilized. Using the equipment software, the diffraction figure was integrated to generate an intensity file as a function of 2θ, the scattering angle, or q, the scattering vector: $q = (4\pi \sin\theta)/\lambda$. The sample-detector distance was 650 mm, which provided a q range between 0.13 nm^{-1} and 3.13 nm^{-1}. The liquid crystalline structures were determined by calculating the values of the interplanar distances, d, from Bragg's law, and these distances were associated with the Miller indices of the structure symmetry.

2.3.3. Light scattering

The mean diameter, particle size distribution, and the zeta potential of the obtained dispersions were determined using dynamic light scattering with a Zetasizer Nano ZS instrument (Malvern Instruments, Worcestershire, UK). The hydrodynamic diameter of the freshly prepared dispersions was measured at 25 °C with a scattering angle of 173° using a He-Ne laser, and the zeta potential was determined by the standard capillary electrophoresis cell of a Zetasizer Nano ZS at 25 °C. The data represent the average values from three separate measurements.

2.4. Screening of in vitro skin penetration of siRNA

After characterization of the nanodispersions, the systems composed of MO/PEI/aqueous phase at 8:2:90 (w/w/w), MO/OAM/aqueous phase at 9.75:0.25:90 (w/w/w), MO/OA/PEI/aqueous phase at 8:2:5:85 (w/w/w), and MO/OA/OAM/aqueous phase at 8:2:2:88 (w/w/w) were selected and added to the GAPDH siRNA-FAM. GAPDH siRNA-FAM was incorporated into the nanodispersions at a final concentration of 10 μM and left for 30 min at room temperature. The systems were then evaluated with regard to their ability to carry the siRNA into the skin to determine which one was the most promising in this regard.

The penetration of siRNA into the skin was assessed using an *in vitro* model of porcine ear skin, as previously described [21]. The skin from the outer surface of a freshly excised porcine ear was carefully dissected and dermatomized at a thickness of 500 μm, stored at −20 °C, and used within 1 month. On the day of the experiment, the skin was thawed and mounted on a Franz diffusion cell (diffusion area of 1.77 cm^2; Hanson Instruments,

Chatsworth, CA) with the stratum corneum facing the donor compartment (where the formulation was applied) and the dermis facing the receptor compartment. The latter compartment was filled with PBS solution (pH 7.4). The receptor phase was under constant stirring and was maintained at 37 ± 0.5 °C during the experiments.

Two hundred microliters of the nanodispersions containing GAPDH siRNA-FAM were applied to the surface of the stratum corneum, corresponding to a dose of 10 μM of GAPDH siRNA-FAM. At 12 h post-application, the skin surfaces were carefully cleaned, and the diffusion area of the skin samples was frozen using acetone at −30 °C, embedded in Tissue-Tek® OCT compound (Pelco International, Redding, CA, USA), and sectioned using a cryostat microtome (Leica, Wetzlar, Germany). The skin sections (10 μm) were mounted on glass slides. The slides were visualized without any additional staining or treatment through a 20X objective using a Zeiss microscope (Axio Imager A.1, Carl Zeiss, Oberkochen, Germany) equipped with a filter for FAM (λ_{exc} = 492 nm and λ_{em} = 517 nm) and AxioVision software. Skin sections treated with 200 μL of PBS or with nuclease-free water solution containing GAPDH siRNA-FAM (10 μM) were used as controls.

2.5. In vivo efficacy

2.5.1. Preparation of nanodispersions

Based on the characterization and *in vitro* skin penetration results, the systems selected for the *in vivo* studies were the nanodispersions composed of MO/OA/PEI/aqueous phase at 8:2:5:85 (w/w/w/w) and MO/OA/OAM/aqueous phase at 8:2:2:88 (w/w/w/w). For the following studies, each nanodispersion was combined with GAPDH siRNA-FAM at 10 μM, mixed gently, and incubated for 30 min at room temperature before use. Different control groups were included during the tests: a PBS-treated group, both nanodispersions with scrambled siRNA-treated groups and a nuclease-free water solution containing GAPDH siRNA-FAM-treated group (referred to in the present study as naked GAPDH siRNA-FAM).

2.5.2. In vivo skin application of nanodispersions in an animal model

In vivo experiments were performed on 3-month-old sex-matched hairless mice of the HRS/J strain housed in a temperature-controlled room with access to water and food *ad libitum*. All of the experiments were conducted in accordance with the National Institutes of Health guidelines for the welfare of experimental animals and with the approval of the Ethics Committee of the Faculty of Pharmaceutical Science of Ribeirao Preto, University of Sao Paulo, Ribeirao Preto, SP, Brazil (Protocol no. 09.1.118.53.2). Randomly chosen animals were divided into groups of 3–5 and were topically treated on the dorsal surface (area ~2 cm^2) with 100 μL of the nanodispersions described above. At 24 and 48 h post-application, the animals were sacrificed with an overdose of carbon dioxide, the surface of the skin was cleaned, and the application area was dissected and analyzed for skin penetration, potential irritation, and the ability to knockdown GAPDH protein levels.

2.5.3. In vivo skin penetration

Some of the hairless skin, treated as explained above (Section 2.5.2), was frozen, sectioned, and analyzed as described for the *in vitro* skin penetration test (Section 2.4).

2.5.4. In vivo skin irritation

Some of the hairless skin, treated as explained above (Section 2.5.2), was frozen using acetone at −30 °C, embedded in Tissue-Tek® OCT compound, and sectioned in 10 μm increments using a cryostat microtome. The skin sections were mounted on glass slides, stained with hematoxylin and eosin (H&E), and examined with a light microscope (Axioplan 2 Image Pol microscope, Carl Zeiss, Oberkochen, Germany). Skin irritation of the studied nanodispersions was evaluated according to established endpoints of infiltration of inflammatory cells and epidermis thickening using the ImageJ Program (NIH, National Institutes of Health).

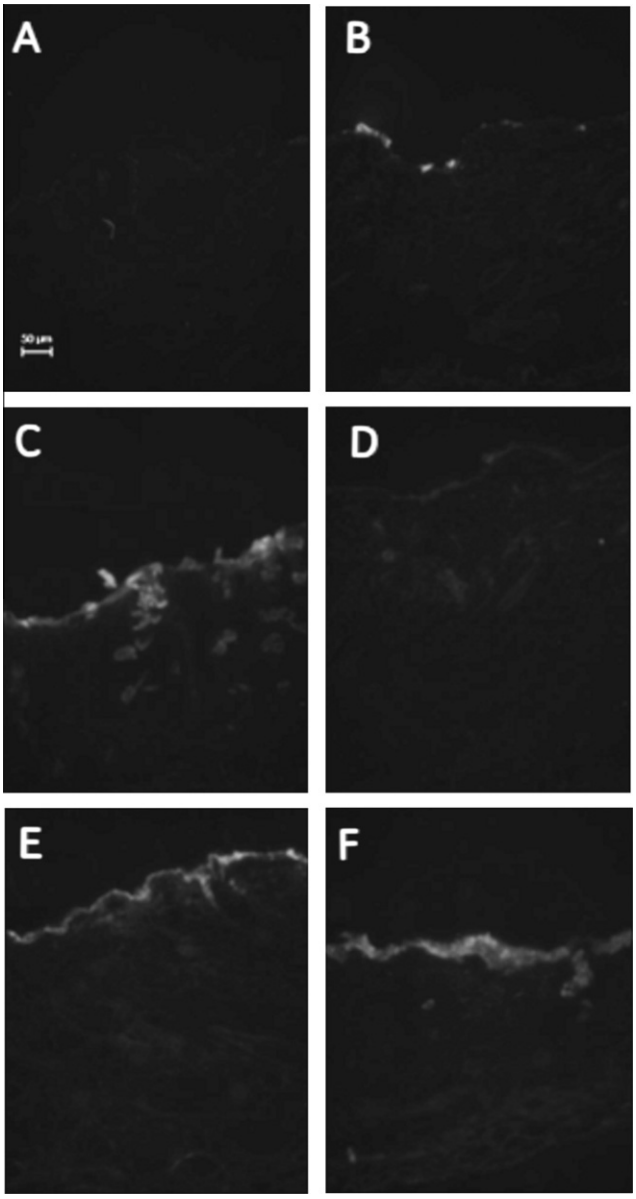

Fig. 3. *In vitro* skin penetration of GAPDH siRNA-FAM. Fluorescence microscopy of porcine ear skin sections after treatment for 12 h with different formulations. (A) PBS; (B) naked GAPDH siRNA-FAM; (C) MO/OAM/aqueous phase (9.75:0.25:90, w/w/w) + GAPDH siRNA-FAM; (D) MO/PEI/aqueous phase (8:2:90, w/w/w) + GAPDH siRNA-FAM; (E) MO/OA/OAM/aqueous phase (8:2:2:88, w/w/w/w) + GAPDH siRNA-FAM; (F) MO/OA/PEI/aqueous phase (8:2:5:85, w/w/w/w) + GAPDH siRNA-FAM. The final concentration of GAPDH siRNA-FAM was 10 μM. The sections were visualized using a FAM filter through a 20X objective. Three batches of each formulation were tested, and representative images are shown.

2.5.5. Suppression of GAPDH protein levels – Western Blot analysis

Some of the hairless skin, treated as described in Section 2.5.2, was homogenized in 50 mM Tris–HCl buffer (pH 7.4) containing 10 mM $CaCl_2$ and 1% protease inhibitor cocktail (1:4, w/w dilution). Whole homogenates were centrifuged at 12,000*g* for 10 min at 4 °C. The protein content was then determined (Bio-Rad Laboratories, CA), and equal amounts of protein (50 μg) were subjected to sodium dodecyl sulfate–polyacrylamide gel electrophoresis (SDS–PAGE) [22], transferred to nitrocellulose membranes (GE Healthcare UK Ltd.) and immunoblotted with 1:1000 anti-GAPDH antibody

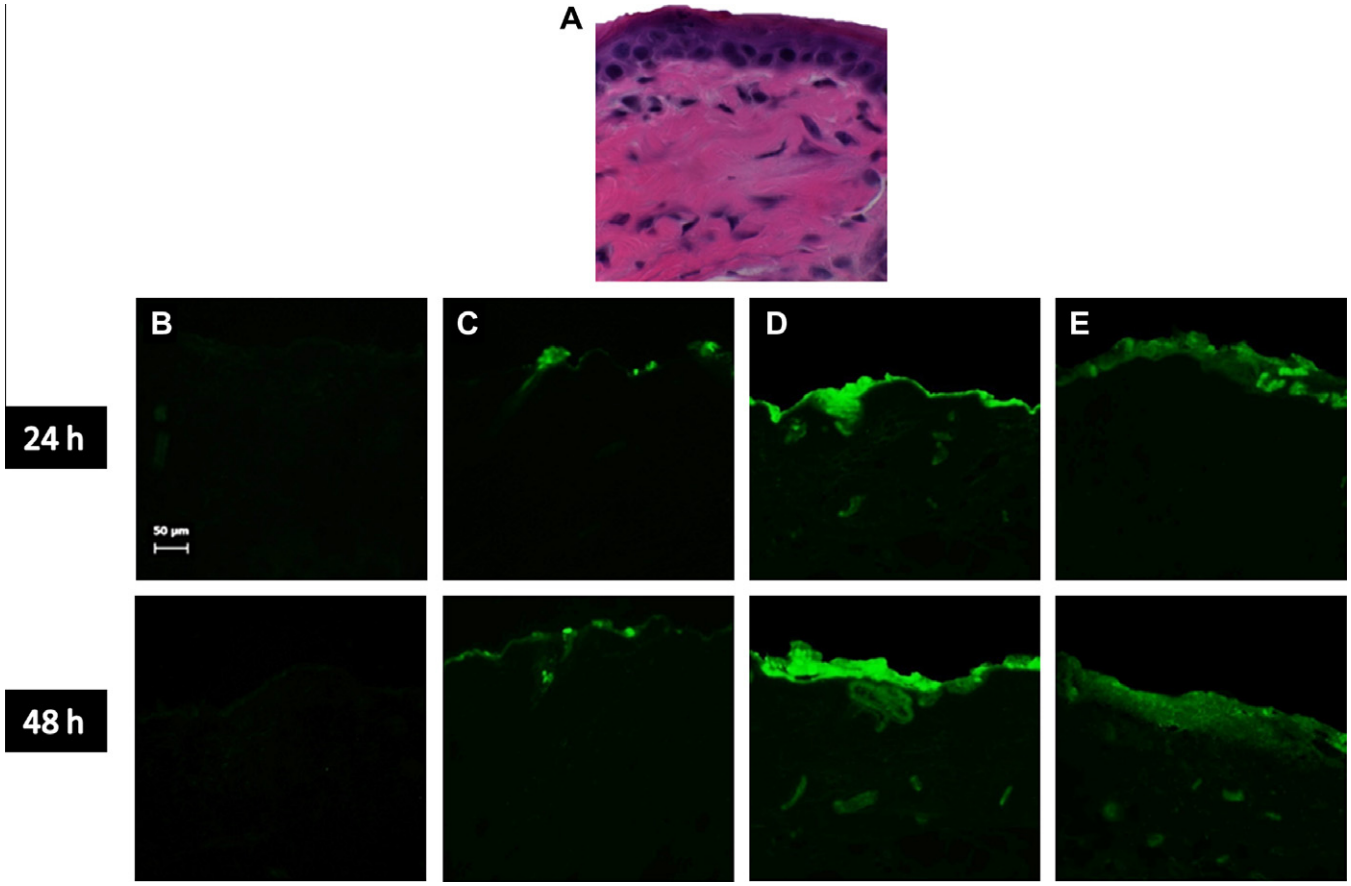

Fig. 4. *In vivo* skin penetration of GAPDH siRNA-FAM. Microscopic evaluation of hairless mouse skin after treatment for 24 and 48 h with different formulations. (A) Light microscopy of skin treated with PBS (H&E). Fluorescence microscopy of skin sections treated with (B) PBS; (C) naked GAPDH siRNA-FAM; (D) MO/OA/OAM/aqueous phase (8:2:2:88, w/w/w/w) + GAPDH siRNA-FAM; and (E) MO/OA/PEI/aqueous phase (8:2:5:85, w/w/w/w) + GAPDH siRNA-FAM. The final concentration of GAPDH siRNA-FAM was 10 μM. The sections were visualized using a FAM filter through a 20X objective. Three batches of each formulation were tested, and representative images are shown. (For interpretation of the references to color in this figure legend, the reader is referred to the web version of this article.)

(FL-335, sc 25778, Santa Cruz Biotechnology). The membranes were subsequently incubated with horseradish peroxidase-conjugated goat anti-rabbit IgG (GE Healthcare, UK Ltd.), and reactive proteins were visualized using ECL Western blotting detection reagents and analysis system (Amersham Biosciences). To ensure equal protein loading, the membranes were stripped and reprobed with anti-β-actin antibodies.

2.6. Statistical analysis

The data were statistically analyzed by one-way ANOVA followed by Bonferroni's multiple comparison *t*-test using GraphPad Prism® software. The results are expressed as the mean ± SEM, and the level of significance was set at $p < 0.05$.

3. Results and discussion

The development of a suitable delivery vehicle capable of increasing the skin penetration of siRNA is of great interest; it is difficult to deliver siRNA into the skin by conventional methods based on passive diffusion because siRNA is a hydrophilic macromolecule [11]. In this report, we propose the use of liquid crystalline phase nanodispersions as a skin delivery system for siRNA.

3.1. Physicochemical properties of the test nanodispersions

Because parameters such as pH, temperature, and the presence of other compounds in the system can influence the packing parameters of lipids and, consequently, liquid crystalline phase formation [23], we first studied whether the cationic polymer PEI or the cationic lipid OAM affected the structure of systems composed of MO/aqueous phase or MO/OA/aqueous phase.

For the MO/aqueous phase systems at 10:90 (w/w), the addition of PEI from 2% to 5% and OAM from 0.25% to 2% changed the liquid crystalline structure from cubic to hexagonal, both with an excess of the aqueous phase. However, for the system composed of MO/OA/aqueous phase at 8:2:90 (w/w/w), the hexagonal structure of the gel containing an excess of aqueous phase was maintained after the addition of different percentages (0.25–5%) of both PEI and OAM. Fig. 1 shows representative images of polarized light microscopy of the liquid crystalline structures obtained by the different systems after the incorporation of PEI or OAM. A fan-like texture, typical of the hexagonal structure, can be observed in Fig. 1E (hexagonal structure with excess of water, composed of MO/OA/OAM/aqueous phase at 8:2:2:88, w/w/w/w).

Lopes et al. [21] obtained a nanodispersion in aqueous medium that retained the internal structure of the bulk phase by dispersing the liquid crystalline system formed by MO and OA in an excess of water in the presence of poloxamer 407 [21]. In the present study, sonication of the different liquid crystalline gels with an excess of aqueous phase resulted in the formation of an anisotropic dispersion, as demonstrated by Fig. 1F.

The SAXS study (Table 1) revealed that the MO-based systems incorporated with PEI did not present a very well organized single cubic phase but contained hexagonal phase interstices. The internal structures of the bulk phase of the other systems were

characterized as single hexagonal structures. In particular, for those containing PEI and OA, we observed a more disordered hexagonal structure. The siRNA incorporation did not influence the liquid crystalline order.

Furthermore, as shown in Fig. 2, the dispersed particles were nanometric (referred to as nanodispersions), as determined by light scattering, and they maintained their diameter (approximately 200 nm) after the addition of siRNA (2.5 μM). The values of the zeta potential varied depending on the final concentration of PEI or OAM incorporated into the system.

Next, based on the characterization study and considering that our aim was to evaluate the potential of liquid crystalline phase nanodispersions as a skin delivery system for siRNA, we chose two different nanodispersions incorporated with OAM in which the hexagonal phase was well-established in addition to two different nanodispersions incorporated with PEI bearing a positive surface charge. Table 2 describes the physicochemical properties of the selected systems after the incorporation of siRNA at 10 μM.

3.2. Screening of the in vitro skin penetration of siRNA

The preliminary studies (Fig. 3) of *in vitro* skin penetration using porcine ear skin mounted in a Franz diffusion cell and visualization by fluorescence microscopy demonstrated that all of the nanodispersions showed increased penetration of GAPDH siRNA-FAM compared with the control formulation, a nuclease-free water solution containing GAPDH siRNA-FAM. However, the presence of OA in the system, a known penetration enhancer [23], influenced the skin permeability, resulting in higher GAPDH siRNA-FAM penetration into deeper skin layers and through tissue. Consequently, the MO/OA-based nanodispersions were selected for further experiments.

3.3. In vivo efficacy of MO/OA/PEI/siRNA/aqueous phase and MO/OA/OAM/siRNA/aqueous phase nanodispersions

3.3.1. In vivo skin penetration

First, the *in vivo* skin penetration of FAM-labeled GAPDH siRNA was assessed by fluorescence microscope visualization at 24 h and 48 h post-application of the selected nanodispersions (Fig. 4). Because the skin presents autofluorescence, skin sections treated with only PBS were used as a control and, as expected, untreated skin presented weak autofluorescence (Fig. 4B). When naked siRNA (nuclease-free water solution containing GAPDH siRNA-FAM at 10 μM) was applied to the skin, FAM-labeled GAPDH siRNA was observed only at specific points on the surface of the skin (Fig. 4C). However, the incorporation of GAPDH siRNA-FAM in MO/OA-based nanodispersions containing either OAM or PEI (Fig. 4D and E, respectively) increased their skin penetration across the stratum corneum, reaching the viable epidermis. There was also an increase in the penetration of GAPDH siRNA-FAM with an increased application time for both nanodispersions.

3.3.2. In vivo skin irritation

Considering that the potential of topical formulations for use as a delivery system should be evaluated not only in terms of carrier capacity and percutaneous drug absorption but also in terms of tolerability and toxicity [24], it is particularly important to consider potential skin irritation resulting from the topical application of the proposed systems (the cationic polymer PEI and the cationic lipid OAM could induce adverse effects depending on the employed concentration). Photomicrographs illustrating skin tissue samples of hairless mice subjected to topical application of the nanodispersions or saline are shown in Fig. 5. No histopathological alterations in the skin of the animals treated with either nanodispersion incorporating GAPDH siRNA-FAM were observed by light microscopy

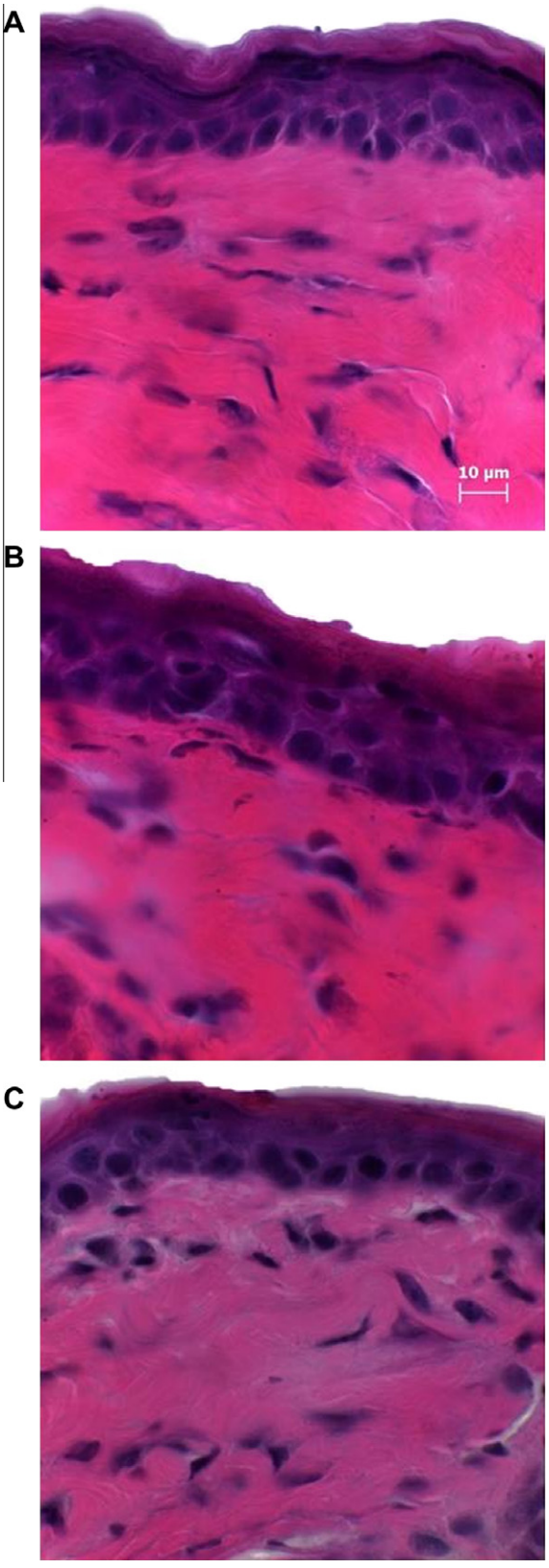

Fig. 5. Photomicrographs of hairless mouse skin sections of animals treated with (A) PBS; (B) MO/OA/OAM/aqueous phase (8:2:2:88, w/w/w/w) + GAPDH siRNA-FAM; and (C) MO/OA/PEI/aqueous phase (8:2:5:85, w/w/w/w) + GAPDH siRNA-FAM for 24 h. The final concentration of GAPDH siRNA-FAM was 10 μM. The sections were stained with H&E and visualized using a conventional light microscope with a 100X objective. (For interpretation of the references to color in this figure legend, the reader is referred to the web version of this article.)

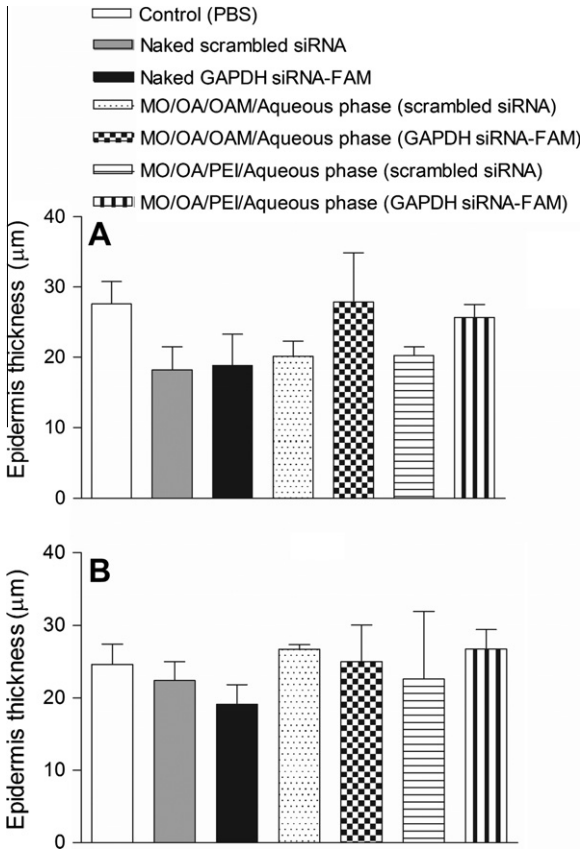

Fig. 6. Epidermis thickness of hairless mouse skin sections at 24 h (A) and 48 h (B) post-application of the different formulations. Both scrambled siRNA and GAPDH siRNA-FAM were added at a final concentration of 10 μM. The results are represented by means ± SEM (n = 3–5). No statistically significant differences were detected.

when compared to the PBS-treated control group. The same results were obtained for the animals treated with naked GADPH-siRNA-FAM, for the nanodispersions with scrambled siRNA-treated groups and for all of the groups examined 48 h post-application (data not shown). Furthermore, as demonstrated by Fig. 6, no significant difference was observed in the epidermal thickness after treatment with the nanodispersions compared to saline-treated animals. Therefore, by evaluating established endpoints for skin irritation (infiltration of inflammatory cells and epidermis thickening), it was demonstrated that the application of the two nanodispersions, under the conditions employed in the present study, did not cause significant skin irritation.

3.3.3. Suppression of GAPDH protein levels

The ability of the carriers to effectively deliver siRNA was investigated in knockdown experiments of the model protein GAPDH. Western blot analysis (Fig. 7) of skin samples 24 and 48 h after application of the MO/OA/PEI/aqueous phase system as carrier of GAPDH siRNA demonstrated marked GAPDH protein reduction (Lane 7) compared with the naked GAPDH siRNA (Lane 3). For the system composed of MO/OA/OAM/aqueous phase, a protein-specific suppression was observed only at 48 h post-treatment (Lane 5). The results also demonstrated that for the PBS control group (Lane 1) and for the scrambled siRNA nanodispersions (Lanes 4 and 6), no knockdown effect was observed.

By comparing the *in vivo* efficacy of the developed nanodispersions, several important conclusions can be made. The nano-scale size of the studied systems may have a great influence on siRNA skin penetration, as it has been suggested that nanostructures

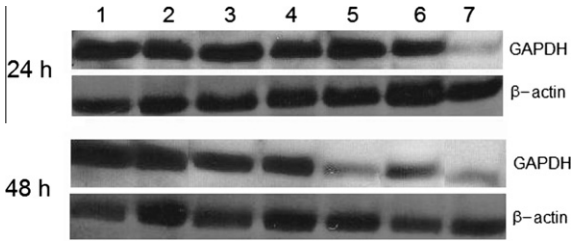

Fig. 7. Silencing of GAPDH protein in hairless mouse skin at 24 and 48 h post-application of the following systems: Lanes: 1 – PBS; 2 – naked scrambled siRNA; 3 – naked GAPDH siRNA-FAM; 4 – MO/OA/OAM/aqueous phase (8:2:2:88, w/w/w/w) + scrambled siRNA; 5 – MO/OA/OAM/aqueous phase (8:2:2:88, w/w/w/w) + GAPDH siRNA-FAM; 6 – MO/OA/PEI/aqueous phase (8:2:5:85 w/w/w/w) + scrambled siRNA; and 7 – MO/OA/PEI/aqueous phase (8:2:5:85 w/w/w/w) + GAPDH siRNA-FAM. Both scrambled siRNA and GAPDH siRNA-FAM were added at a final concentration of 10 μM. The data are representative of three independent experiments with 3–5 animals per group.

are more likely to interact with the stratum corneum and enable siRNA to access to the living cells within the epidermis and dermis [25].

Additionally, the different biological activities of the two nanodispersions studied might be partially controlled by their physicochemical surface properties (zeta-potentials). Considering that prior to cellular uptake, nanoparticles will interact with components of the cellular membrane and that it is generally accepted that the uptake of nanoparticles bearing a positive surface charge will be facilitated by electrostatic interactions with negatively charged cell membranes [19], the highest zeta potential observed for the PEI-based nanodispersion may have greatly influenced carrier uptake.

Finally, liquid crystalline nanodispersions present interesting properties for use as topical delivery systems of siRNA: (i) the presence of the penetration enhancers MO and OA, which facilitate siRNA penetration across the stratum corneum and deeper skin layers; (ii) the ability to protect the siRNA from physical and enzymatic degradation; and (iii) the capability to form a deposit on the skin surface and appendages, resulting in a prolonged release of the incorporated compound [21]. This last feature might eventually translate into different siRNA penetration profiles and might explain the biological activity observed only at 48 h post-application of the MO/OA/OAM/siRNA/aqueous phase nanodispersion, which showed a well-structured hexagonal phase.

Nevertheless, as proven by a previous study of our group in which we observed that a liquid crystalline nanodispersion was more effective than a bulk gel with the same lipid composition [21], for macromolecule topical delivery systems, it is not only the presence of permeation enhancer compounds and the liquid crystalline structure that are responsible for the observed efficacy of the nanodispersions as siRNA delivery systems but the system as a whole.

4. Conclusion

The present work developed optimized hexagonal phase nanoparticles dispersed in aqueous medium presenting interesting properties, which enabled their use as skin delivery system of siRNA. To our knowledge, this report is the first to demonstrate the potential of such systems as siRNA carriers into the skin, and because the *in vivo* delivery of siRNA still represents a major hurdle for any therapeutic intervention, these nanodispersions may represent a promising new possibility for a non-viral vehicle. Furthermore, they can be considered highly advantageous in the treatment of skin disorders, as the developed nanodispersions showed increased siRNA skin penetration and cellular uptake with enhanced biological activity, without causing skin irritation.

Further studies will be pursued to verify if the changes in the proposed systems' composition, dosing frequency, siRNA concentration, and other parameters can optimize the efficacy of siRNA in targeting skin disease-specific gene expression.

Acknowledgments

We thank Dr. Daniel de Paula (Unicentro, Brazil) for helpful discussions and Dimitrius L. Pitol and Nilce O. Wolga for technical assistance. We also thank Prof. Mamie Mizusaki Iyomasa for histological test. This work was supported by "Fundação de Amparo à Pesquisa do Estado de São Paulo" (FAPESP, Brazil, project # 04/09465-7) and "Conselho Nacional de Pesquisa" (CNPq, Brazil). F.T.M.C. Vicentini was the recipient of a FAPESP fellowship (Process # 09/00332-8).

References

[1] D. De Paula, M.V. Bentley, R.I. Mahato, Hydrophobization and bioconjugation for enhanced siRNA delivery and targeting, RNA 13 (4) (2007) 431–456.
[2] E. Gonzalez-Gonzalez, H. Ra, R.P. Hickerson, Q. Wang, W. Piyawattanametha, M.J. Mandella, G.S. Kino, D. Leake, A.A. Avilion, O. Solgaard, T.C. Doyle, C.H. Contag, R.L. Kaspar, SiRNA silencing of keratinocyte-specific GFP expression in a transgenic mouse skin model, Gene Ther. 16 (8) (2009) 963–972.
[3] A.R. de Fougerolles, Delivery vehicles for small interfering RNA in vivo, Hum. Gene Ther. 19 (2) (2008) 125–132.
[4] M. Takanashi, K. Oikawa, K. Sudo, M. Tanaka, K. Fujita, A. Ishikawa, S. Nakae, R.L. Kaspar, M. Matsuzaki, M. Kudo, M. Kuroda, Therapeutic silencing of an endogenous gene by siRNA cream in an arthritis model mouse, Gene Ther. 16 (8) (2009) 982–989.
[5] M.A. Tran, R. Gowda, A. Sharma, E.J. Park, J. Adair, M. Kester, N.B. Smith, G.P. Robertson, Targeting V600EB-Raf and Akt3 using nanoliposomal-small interfering RNA inhibits cutaneous melanocytic lesion development, Cancer Res. 68 (18) (2008) 7638–7649.
[6] V.D. Thanik, M.R. Greives, O.Z. Lerman, N. Seiser, W. Dec, C.C. Chang, S.M. Warren, J.P. Levine, P.B. Saadeh, Topical matrix-based siRNA silences local gene expression in a murine wound model, Gene Ther. 14 (17) (2007) 1305–1308.
[7] P. Ritprajak, M. Hashiguchi, M. Azuma, Topical application of cream-emulsified CD86 siRNA ameliorates allergic skin disease by targeting cutaneous dendritic cells, Mol. Ther. 16 (7) (2008) 1323–1330.
[8] S.A. Leachman, R.P. Hickerson, P.R. Hull, F.J. Smith, L.M. Milstone, E.B. Lane, S.J. Bale, D.R. Roop, W.H. McLean, R.L. Kaspar, Therapeutic siRNAs for dominant genetic skin disorders including pachyonychia congenita, J. Dermatol. Sci. 51 (3) (2008) 151–157.
[9] M. Nakamura, J. Jo, Y. Tabata, O. Ishikawa, Controlled delivery of T-box21 small interfering RNA ameliorates autoimmune alopecia (Alopecia Areata) in a C3H/HeJ mouse model, Am. J. Pathol. 172 (3) (2008) 650–658.
[10] M. Jakobsen, K. Stenderup, C. Rosada, B. Moldt, S. Kamp, T.N. Dam, T.G. Jensen, J.G. Mikkelsen, Amelioration of psoriasis by anti-TNF-alpha RNAi in the xenograft transplantation model, Mol. Ther. 17 (10) (2009) 1743–1753.
[11] K. Kigasawa, K. Kajimoto, S. Hama, A. Saito, K. Kanamura, K. Kogure, Noninvasive delivery of siRNA into the epidermis by iontophoresis using an atopic dermatitis like model rat, Int. J. Pharm. 383 (1) (2010) 157–160.
[12] T. Hsu, S. Mitragotri, Delivery of siRNA and other macromolecules into skin and cells using a peptide enhancer, Proc. Natl. Acad. Sci. USA 108 (38) (2011) 15816–15821.
[13] S.Y. Wu, N.A. McMillan, Lipidic systems for in vivo siRNA delivery, AAPS J. 11 (4) (2009) 639–652.
[14] K.A. Howard, S.R. Paludan, M.A. Behlke, F. Besenbacher, B. Deleuran, J. Kjems, Chitosan/siRNA nanoparticle-mediated TNF-alpha knockdown in peritoneal macrophages for anti-inflammatory treatment in a murine arthritis model, Mol. Ther. 17 (1) (2009) 162–168.
[15] F. Pittella, M. Zhang, Y. Lee, H.J. Kim, T. Tockary, K. Osada, T. Ishii, K. Miyata, N. Nishiyama, K. Kataoka, Enhanced endosomal escape of siRNA-incorporating hybrid nanoparticles from calcium phosphate and PEG-block charge-conversional polymer for efficient gene knockdown with negligible cytotoxicity, Biomaterials 32 (11) (2011) 3106–3114.
[16] G. Cevc, U. Vierl, Nanotechnology and the transdermal route: a state of the art review and critical appraisal, J. Control Release 141 (3) (2010) 277–299.
[17] C.A. Fernandez, K.G. Rice, Engineered nanoscaled polyplex gene delivery systems, Mol. Pharm. 6 (5) (2009) 1277–1289.
[18] X.B. Xiong, H. Uludag, A. Lavasanifar, Biodegradable amphiphilic poly(ethylene oxide)-block-polyesters with grafted polyamines as supramolecular nanocarriers for efficient siRNA delivery, Biomaterials 30 (2) (2009) 242–253.
[19] A.J. Convertine, D.S. Benoit, C.L. Duvall, A.S. Hoffman, P.S. Stayton, Development of a novel endosomolytic diblock copolymer for siRNA delivery, J. Control Release 133 (3) (2009) 221–229.
[20] D. Libster, A. Aserin, N. Garti, Interactions of biomacromolecules with reverse hexagonal liquid crystals: drug delivery and crystallization applications, J. Colloid Interface Sci. 356 (2) (2011) 375–386.
[21] L.B. Lopes, D.A. Ferreira, D. de Paula, M.T. Garcia, J.A. Thomazini, M.C. Fantini, M.V. Bentley, Reverse hexagonal phase nanodispersion of monoolein and oleic acid for topical delivery of peptides: in vitro and in vivo skin penetration of cyclosporin A, Pharm. Res. 23 (6) (2006) 1332–1342.
[22] U.K. Laemmli, Cleavage of structural proteins during the assembly of the head of bacteriophage T4, Nature 227 (5259) (1970) 680–685.
[23] L.B. Lopes, J.L. Lopes, D.C. Oliveira, J.A. Thomazini, M.T. Garcia, M.C. Fantini, J.H. Collett, M.V. Bentley, Liquid crystalline phases of monoolein and water for topical delivery of cyclosporin A: characterization and study of in vitro and in vivo delivery, Eur. J. Pharm. Biopharm. 63 (2) (2006) 146–155.
[24] F.T. Vicentini, T.R. Simi, J.O. Del Ciampo, N.O. Wolga, D.L. Pitol, M.M. Iyomasa, M.V. Bentley, M.J. Fonseca, Quercetin in w/o microemulsion: in vitro and in vivo skin penetration and efficacy against UVB-induced skin damages evaluated in vivo, Eur. J. Pharm. Biopharm. 69 (3) (2008) 948–957.
[25] X. Wu, G.J. Price, R.H. Guy, Disposition of nanoparticles and an associated lipophilic permeant following topical application to the skin, Mol. Pharm. 6 (5) (2009) 1441–1448.